

Effects of biomechanical forces on signaling in the cortical collecting duct (CCD)

Rolando Carrisoza-Gaytan,¹ Yu Liu,² Daniel Flores,^{2,3} Cindy Else,¹ Heon Goo Lee,⁴ George Rhodes,⁵ Ruben M. Sandoval,⁵ Thomas R. Kleyman,⁶ Francis Young-In Lee,⁴ Bruce Molitoris,⁵ Lisa M. Satlin,^{1,2,*} and Rajeev Rohatgi^{1,2,3,*}

¹Department of Pediatrics, Icahn School of Medicine at Mount Sinai, New York, New York; ²Department of Medicine, Icahn School of Medicine at Mount Sinai, New York, New York; ³Department of Medicine, James J. Peters Veterans Affairs Medical Center, New York, New York; ⁴Department of Orthopedics, Robert Carroll and Jane Chace Carroll Laboratories, Columbia College of Physicians and Surgeons, New York, New York; ⁵Department of Medicine, Indiana University School of Medicine, Indianapolis, Indiana; and ⁶Department of Medicine, University of Pittsburgh School of Medicine, Pittsburgh, Pennsylvania

Submitted 2 December 2013; accepted in final form 19 May 2014

Carrisoza-Gaytan R, Liu Y, Flores D, Else C, Lee HG, Rhodes G, Sandoval RM, Kleyman TR, Lee FY, Molitoris B, Satlin LM, Rohatgi R. Effects of biomechanical forces on signaling in the cortical collecting duct (CCD). *Am J Physiol Renal Physiol* 307: F195–F204, 2014. First published May 28, 2014; doi:10.1152/ajprenal.00634.2013.—An increase in tubular fluid flow rate (TFF) stimulates Na reabsorption and K secretion in the cortical collecting duct (CCD) and subjects cells therein to biomechanical forces including fluid shear stress (FSS) and circumferential stretch (CS). Intracellular MAPK and extracellular autocrine/paracrine PGE₂ signaling regulate cation transport in the CCD and, at least in other systems, are affected by biomechanical forces. We hypothesized that FSS and CS differentially affect MAPK signaling and PGE₂ release to modulate cation transport in the CCD. To validate that CS is a physiological force *in vivo*, we applied the intravital microscopic approach to rodent kidneys *in vivo* to show that saline or furosemide injection led to a 46.5 ± 2.0 or $170 \pm 32\%$ increase, respectively, in distal tubular diameter. Next, murine CCD (mpkCCD) cells were grown on glass or silicone coated with collagen type IV and subjected to 0 or 0.4 dyne/cm² of FSS or 10% CS, respectively, forces chosen based on prior biomechanical modeling of *ex vivo* microperfused CCDs. Cells exposed to FSS expressed an approximately twofold greater abundance of phospho(p)-ERK and p-p38 vs. static cells, while CS did not alter p-p38 and p-ERK expression compared with unstretched controls. FSS induced whereas CS reduced PGE₂ release by ~40%. In conclusion, FSS and CS differentially affect ERK and p38 activation and PGE₂ release in a cell culture model of the CD. We speculate that TFF differentially regulates biomechanical signaling and, in turn, cation transport in the CCD.

stretch; fluid shear stress; flow; MAPK; prostaglandin E₂; collecting duct

INCREASES IN URINARY FLOW rate, as following volume expansion or diuretic administration, subject epithelial cells in the distal nephron, which includes the cortical collecting duct (CCD), to fluid shear stress (FSS) and circumferential stretch (CS) acting parallel and perpendicular, respectively, to the tubular wall, as well as drag/torque on apical cilia of Na-absorbing principal cells and microvilli/microplicae of acid-base-transporting intercalated cells therein (8, 11, 23, 39). In the isolated perfused CCD, these hydrodynamic forces are transduced into increases

in intracellular Ca²⁺ concentration ([Ca²⁺]_i) (23, 39) and autocrine/paracrine release of PGE₂ (13, 20), effectors that activate iberiotoxin (IbTX)-sensitive apical voltage- and Ca²⁺-activated BK channels in principal cells that mediate flow-induced K secretion (FIKS) (5, 22, 23, 29, 30, 34, 40, 41). Apical BK channels appear to be tonically inhibited under low-flow conditions by MAPKs (17) and PKA (22), suggesting that FIKS, if mediated by principal cells, requires release of channel inhibition directly or indirectly by these kinases.

It is well established that the central cilium serves as a mechanosensor, transducing mechanical manipulation (either directly or induced by urinary flow) into an increase in [Ca²⁺]_i in renal epithelial cells (23, 26, 31–33). However, it is uncertain as to whether FSS and/or CS is physiologically relevant *in vivo*. The FSS experienced by renal distal tubular cells in the native kidney is unknown. Also uncertain is whether the 15–20% increase in tubular diameter observed in microperfused CCDs subject to an acute increase in tubular flow rate (23), if extrapolated to the full complement of CCDs in the native kidney, is possible; the anticipated increase in renal volume may be prevented by the nondistensible renal capsule. However, *in vivo* multiphoton microscopy studies of Ca²⁺ fluorophore-loaded intact mouse kidneys revealed increases in CD tubular diameter in response to increases in tubular flow, although the magnitude of the increases in diameter was not reported (37).

The purpose of the current study was to identify whether FSS and/or CS is a physiologically relevant hydrodynamic force in the distal nephron and to examine whether these discrete forces activate distinct signaling pathways in the distal nephron. To test this, we performed intravital imaging in intact rodent kidney to measure the magnitude of flow-induced increases in distal nephron diameter *in vivo* and, based on these results, examined the effects of FSS and CS applied to monolayers of CCD cells on activation of MAPK and PGE₂ signaling pathways, both reported to influence FIKS in the CCD (17, 22).

MATERIALS AND METHODS

Intravital Imaging of Rat Distal Nephron

Animal studies were conducted in conformity with the National Institutes of Health *Guide for the Care and Use of Laboratory Animals* and approved by the Animal Care and Use Committee at the

* L. M. Satlin and R. Rohatgi contributed equally to this work.

Address for reprint requests and other correspondence: R. Rohatgi, One Gustave L. Levy Place, Box 1664, The Mount Sinai School of Medicine, New York, NY 10029 (e-mail: rajeev.rohatgi@mssm.edu).

Indiana University School of Medicine. Sprague-Dawley rats were anesthetized with pentobarbital sodium (50 mg/ml; 0.15 ml/100 g). The internal jugular vein was cannulated, and the left kidney was exteriorized, placed onto a coverslip bottom dish filled with warm normal saline, and imaged on an inverted multiphoton microscope using a $\times 60$ water-immersion objective (NA 1.2) (4, 10). Studies were performed using either a Bio-Rad MRC-1024MP Laser-Scanning Confocal/Multiphoton scanner (Hercules, CA) attached to a Nikon Diaphot inverted microscope (Fryer, Huntley, IL) or an Olympus FV1000 microscope adapted for two-photon microscopy, as previously described (10, 35). Hoechst 33342 was infused into animals intravenously (iv) to label nuclei, and small 3-kDa dextrans conjugated to either Texas red or cascade blue fluorophores were infused to mark the lumens of the tubule. Distal tubules were distinguished from proximal tubules as the latter are easily identified by their robust internalization of fluorescent dextrans into endocytic compartments (4, 10). The microvasculature was identified by the iv infusion of a large 500-kDa fluorescein dextran (4, 10).

Imaging was initially performed to identify the greatest diameter of the distal tubule. Thereafter, animals were injected iv with either 1 mg/kg furosemide (over 2 min) or isotonic saline (2% of total body weight; ~ 5 ml in a 250-g rat). A second 3-kDa fluorescent dextran was rapidly infused while the same XY plane of visualization was maintained. The change in diameter of the tubule, imaged before and during the diuresis, was measured in each distal tubule using Metamorph v7 (Molecular Devices, Sunnyvale, CA). The change in diameter was averaged for each tubule.

Cell Culture

Murine immortalized mpk CCD (mpkCCD) cells were grown in DMEM:Ham's F12 (with 60 nM sodium selenate, 5 μ g/ml transferrin, 2 mM glutamine, 50 nM dexamethasone, 1 nM tri-iodothyronine, 10 ng/ml epidermal growth factor, 5 μ g/ml insulin, 20 mM D-glucose, 2% fetal calf serum, and 20 mM HEPES) on 25 \times 75-mm glass slides or collagen type IV-coated silicone supports (Flexcell, Hillsborough, NC). Experiments were performed once the cell monolayers reached confluence (3–4 days on glass and 7 days on silicone). Cells were used only up to *passage 15* due to the risk of genetic drift.

Immunocytochemistry

To ensure that mpkCCD cells grown on glass and silicone supports had achieved similar stages of differentiation at the time of study, cell number/density and morphology were examined using an immunofluorescence approach. Specifically, antibodies directed against occludin and zonula occludins (ZO)-1 were utilized to localize these tight junction proteins, rhodamine-phalloidin to identify F-actin, and 4,6-diamidino-2-phenylindole (DAPI) to label nuclei. Confluent monolayer of cells were fixed with 2.5% paraformaldehyde diluted in PBS at 4°C, permeabilized with 0.3% Triton X-100 at room temperature (RT), and blocked with a 1% BSA/10% goat serum (GS) solution at RT. Antibodies (see *Reagents*) were diluted in a 0.1% Triton X-100, 0.1% BSA, and 1% GS PBS solution applied overnight at 4°C, and corresponding secondary antibodies were applied for 1 h at RT. After each antibody incubation, monolayers were washed three times with PBS-T (0.1% Triton X-100 in PBS) at RT for 5 min. Control experiments were performed in the absence of primary antibody but in the presence of secondary antibody. Cell monolayers were mounted on glass slides with an antifade reagent and visualized with a Leica SP5 DM Confocal Laser-Scanning Microscope.

Exposure of mpkCCD Cells to Hydrodynamic Forces

Confluent monolayers of mpkCCD cells, grown on glass slides (for FSS) or collagen type IV-coated silicone supports (for CS), were made serum and additive free for 2 h before exposure to FSS or CS. At the conclusion of each experiment, control and experimental

(subject to FSS or CS) were fixed for immunofluorescence analyses or protein lysate generated for immunoblotting.

FSS. Monolayers of cells grown on glass slides or collagen type IV-coated glass slides were placed in a laminar flow chamber (Glycotech), maintained at 37°C, and subject to shear of 0.4 dyne/cm² for varying durations using phenol red-free, serum-free DMEM/F12. This level of FSS was selected as we have previously reported that CCDs experience a FSS of ~ 0.4 dyne/cm² when perfused at a fast physiological flow rate of 5 nl·min⁻¹·mm⁻¹ (23). FSS was calculated based on Poiseuille's law; $\tau = \mu\gamma = 6\mu Q/a^2b$, where τ = wall stress (dyne/cm²), γ = shear rate (per s), μ = apparent viscosity of the fluid (media at 37°C = 0.76 cP), a = channel height of a rectangular flow chamber (cm), b = channel width of a rectangular flow chamber (cm), and Q = volumetric rate (ml/s). Static control cells were exposed to the same solutions and duration as sheared cells, but without exposure to FSS.¹

Stretch. Monolayers of cells on silicone supports to be stretched were placed in a vacuum-assisted Flexcell FX 5000T System (Flexcell), housed in a humidified 37°C incubator injected with 95% O₂ and 5% CO₂, while control unstretched cells were housed in an identical incubator without the Flexcell system. Equal volumes of fresh serum- and additive-free DMEM/F12 media were placed in the wells containing the mpkCCD cells. Cells were exposed to either constant 10% equibiaxial stretch for 30 min or maintained under static/unstretched conditions. This time interval was chosen as in vitro microperfused tubules subject to an acute increase in luminal flow rate exhibit an increase in tubular diameter (to ~ 15 – 20%) and onset of sustained FIKS within 10 min (22, 23, 40). Media and cells were collected at the end of each experiment for measurement of PGE₂ concentration following the protocol of the PGE₂ EIA Assay Kit (Cayman Chemical) (13); this value was normalized to total cellular protein.

Immunoblotting To Assess Mechanoactivation of MAPK

Western blot analysis was performed as previously described (12). Cell protein lysates (30–50 μ g) were isolated, resolved electrophoretically, and transferred to Immobilon filters (Millipore, Billerica, MA). Filters were blocked in 5% nonfat dry milk and 0.1% Tween and immunoblotted with a primary antibody (see *Reagents*). After washing, blots were incubated with a horseradish peroxidase-conjugated secondary antibody (Sigma, St. Louis, MO), and bands were visualized by a West Pico enhanced chemiluminescence kit (Pierce, Rockford, IL). After the membrane was stripped and blocked, the blot was incubated with an anti-total protein-specific antibody and visualized using the same methods as the primary antibody. Densitometric analysis was performed on the pERK and total ERK doublet, while two densitometric analyses were performed on the p38 signal: 1) the single bottom band, identical in molecular weight to that of total p38 and 2) both bands. Both analyses were performed because p38 has four known isoforms of varying molecular weights: α , β , γ , and δ . The anti-p38 antibody we used in the study recognizes α , β , and γ .

Cell Viability

Cells were trypsinized, collected, centrifuged, and then resuspended in 2 ml of serum-free media. A 0.4% solution of trypan blue (Corning/Cellgro, Tewksbury, MA) diluted in serum-free media was incubated with 0.2 ml of the cell suspension. The total numbers of cells and viable cells were counted by a hemocytometer from two

¹ While one might suggest that a low FSS would be a more appropriate control than static conditions, we propose that comparison of high vs. no FSS is also justified because biomechanical signaling in renal epithelial cells occurs only after FSS exceeds a threshold. For example, we have reported in split-open mammalian CCDs that an increase in superfusate flow from 0 to 3.2 μ l/s failed to generate a [Ca²⁺]_i response. However, an increase in superfusate flow from 3.2 to 25 μ l/s triggered a significant increase in [Ca²⁺]_i in both principal and intercalated cells (23). Because, 0 and 3.2 μ l/s generated equivalent responses, we considered that the static condition was an adequate control.

samples of the cell suspension and averaged. Viability was expressed as the percentage of viable cells to the total number of cells.

Reagents

Antibodies (final concentration) used included rabbit anti-ERK (1:1,000, Cell Signaling), rabbit anti-pERK (1:1,000, Cell Signaling), rabbit anti-p38 (1:500, Cell Signaling), rabbit anti-p-p38 (1:500, Cell Signaling), rabbit anti-ZO-1 (1:100, Abcam), rabbit anti-occludin (1:50, Abcam), and goat anti-rabbit conjugated to horseradish peroxidase (1:5,000, Sigma) for immunoblotting or goat anti-rabbit conjugated to Alexa 488 (1:200, Molecular Probes) for immunofluorescence. Other labels used for immunolabeling were rhodamine-phalloidin (1:40, Molecular Probes) and ProLong Gold Antifade Reagent with DAPI (Molecular Probes). Intravital reagents included 500-kDa fluorescein dextran, cascade blue/fluorescein- or Texas red-labeled 3-kDa dextrans, and Hoechst 33342 (Life Technologies/Molecular Probes).

Statistics

Data are given as means \pm SE (n = number of slides or silicone supports). Statistical analyses were performed using paired t -tests for the intravital imaging studies and unpaired t -tests for cell culture experiments (SigmaPlot, version 11.0).

RESULTS

High TFF Is Accompanied by CS In Vivo

To discern the magnitude of CS experienced by the distal nephron in the native kidney in response to a diuresis, we performed multiphoton intravital microscopy of rodent kidneys

before and after intravenous injection of saline or furosemide. Small-molecular-weight dextrans (3-kDa), conjugated to either Texas red or cascade blue, are freely filtered by the glomerulus and are endocytosed by the proximal tubule, which are then easily identified by the accumulation of the fluorophore at the brush border (Fig. 1). Tubules that do not endocytose the dextran but label brightly with Hoechst (nuclei) are distal tubules (Fig. 1) (10). In three rats, volume expansion with saline led to a $46.5 \pm 2.0\%$ increase in tubular diameter, from 18.3 ± 2.7 to $25.6 \pm 4.2 \mu\text{m}$ ($P < 0.05$). In another three rats, administration of 1 mg/kg furosemide led to a $170 \pm 32\%$ increase in tubular diameter from 11.6 ± 0.7 to $30.0 \pm 3.1 \mu\text{m}$ ($P < 0.05$) (Fig. 1). These data indicate that an acute increase in urinary flow rate in the distal nephron, generated by saline or furosemide administration, leads to CS in the native kidney with an intact capsule.

mpkCCD Monolayer Integrity

Because the cellular supports for FSS experiments (rigid glass) differed from those used for stretch (flexible collagen type IV-coated silicone), we sought to define growth conditions that would ensure that all mpkCCD cell monolayers studied were morphologically similar. Cells grown on silicone supports grew more slowly than those grown on glass. To ensure that a comparable degree of cellular differentiation was achieved in cells on glass and silicone before study, nuclei were stained with DAPI and counted within a defined field

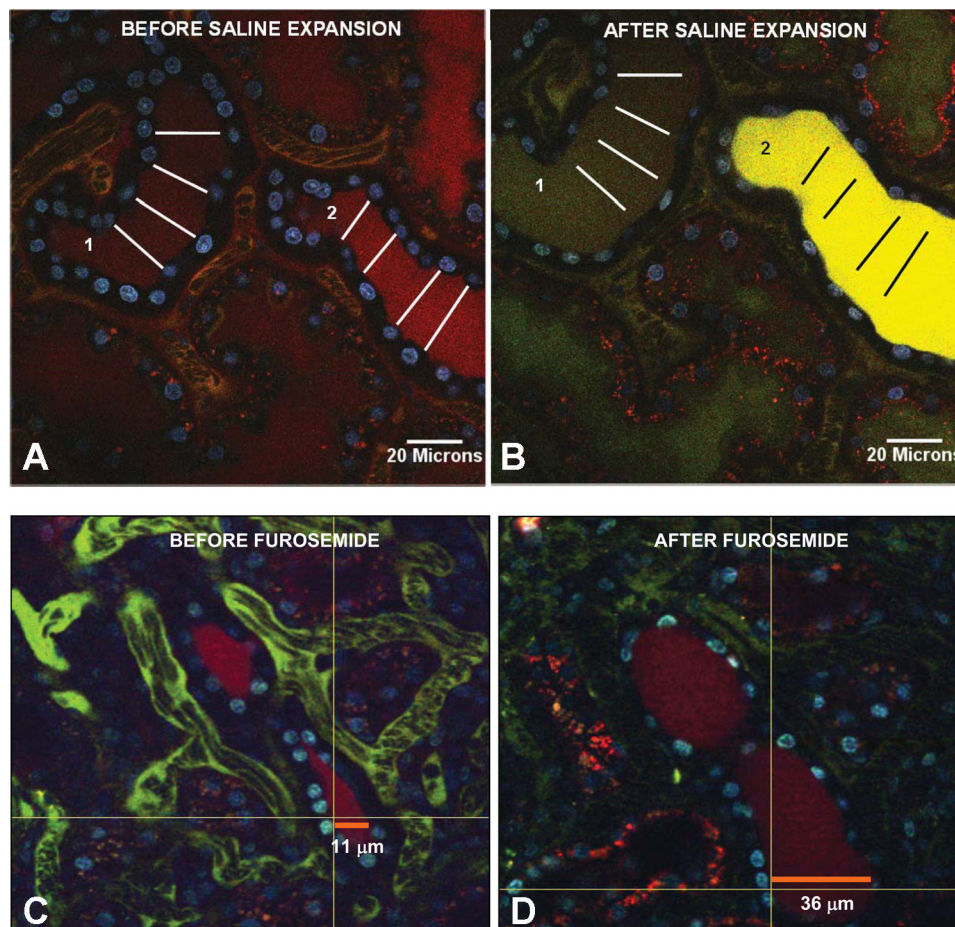


Fig. 1. Two-photon imaging of superficial rat kidney before and during intravascular saline expansion or furosemide administration. Distal tubules are identified by the bright labeling of the nuclei therein with 4,6-diamidino-2-phenylindole (DAPI; blue) and the absence of endocytosis of dextran conjugated to Texas red. *A*: before volume expansion, the mean diameters for tubules 1 and 2 were 25.5 ± 1.4 and $21.9 \pm 2.9 \mu\text{m}$, respectively. *B*: after intravascular volume expansion with a 5-ml saline bolus, a 3-kDa fluorescein dextran (green) was rapidly infused. The bars in *A* are superimposed onto the image of the same tubules after volume expansion in *B*, showing the significant increases in diameter of both tubules. *C* and *D*: a similar experiment was performed, except that this rat was injected with 1 mg/kg furosemide instead of saline. *C*: before furosemide, the diameter of the distal tubule in the focal plane shown and identified by the orange bar was $11 \mu\text{m}$. *D*: after furosemide infusion, the diameter of the distal tubule increased to $36 \mu\text{m}$.

under a $\times 63$ objective. Based on these analyses, cell number was found to be similar in monolayers grown for 3–4 days on glass and 7 days on silicone. To confirm that cell size, tight junction complex, and actin cytoskeleton were also similar in monolayers subject to FSS and CS, and to test whether FSS or CS differentially induced localization of tight junctional proteins, immunolabeling was performed for occludin, ZO-1, and F-actin. Under static (no FSS or CS) conditions, the plasma membrane localization of occludin (Fig. 2, *A* and *C*) and ZO-1 (Fig. 2, *E* and *G*) did not differ between cells grown on glass $\times 4$ days or collagen IV coated-silicone $\times 7$ days. Neither FSS nor CS altered the localization of occludin (Fig. 2, *B* and *D*) or ZO-1 (Fig. 2, *F* and *H*) compared with static controls. Similarly, the location of F-actin in the apical membrane was similar in cells grown on glass (Fig. 2*I*) and silicone (Fig. 2*K*), and neither FSS nor CS affected its apical localization (Fig. 2, *J* and *L*). F-actin at the basolateral membrane also did not differ between cells grown on glass (Fig. 2*M*) and silicone (Fig. 2*O*) under static conditions; however, FSS induced an increase in basolateral stress fibers (Fig. 2*N*) while CS enhanced F-actin expression at the lateral membranes (Fig. 2*P*), suggesting that discrete biomechanical forces lead to unique structural cell responses.

FSS Stimulates MAPK in mpkCCD Cells

Because 1) an increase in tubular fluid flow rate activates BK channel-mediated FIKS and 2) ERK and p38 MAPK tonically suppress apical BK channel activity in principal

cells (17), we sought to test the hypothesis that FSS influences ERK and p38 phosphorylation in mpkCCD cells. To examine this, cells grown on glass slides or collagen IV-coated glass slides were exposed to static conditions (control) or to a physiological level of FSS (0.4 dyne/cm²) for variable time intervals (1–60 min), and Western blotting was performed to detect phospho-ERK (pERK), phospho-p38 (p-p38), total ERK, and total p38. FSS rapidly stimulated phosphorylation of ERK, within 3 min in cells grown on glass slides, a response that was sustained for up to 60 min of FSS (Fig. 3, *A* and *B*). In cells grown on collagen IV-coated glass slides, FSS did not induce pERK expression at 10 min, but by 30 min FSS, expressed $\sim 60\%$ more pERK than static cells (Fig. 3*C*). Similarly, FSS led to a rapid increase in abundance of phosphorylated p38 (Fig. 4, *A* and *B*) in mpkCCD cells grown on glass slides (Fig. 4, *A* and *B*) and collagen IV-coated glass slides (Fig. 4*C*).

CS Differentially Affects MAPK Activation in mpkCCD Cells

Since our ex vivo microperfusion (23) and in vivo intravital experiments (Fig. 1) identified an increase in CS with an increase in tubular fluid flow rate and diuresis, respectively, we sought to examine whether CS stimulated the same signaling pathways induced by FSS. mpkCCD cells grown on collagen IV-coated silicone supports $\times 7$ days were exposed to constant, nonpulsatile stretch (10%) for 30 min, a stretch stimulus similar in magnitude to that observed in the ex vivo microperfused CCD (and associated with activation of FIKS). Immu-

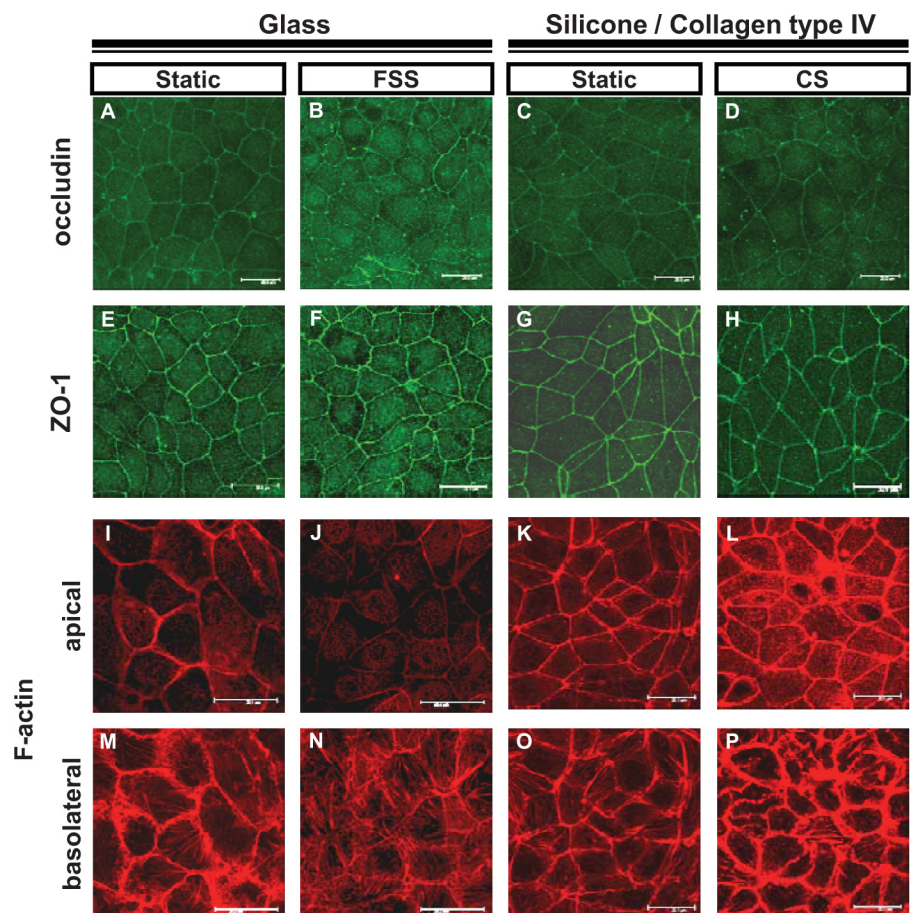
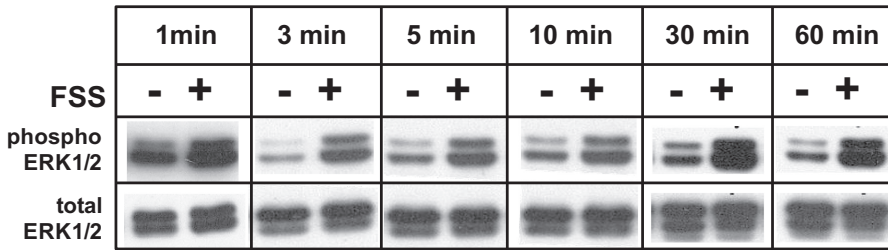
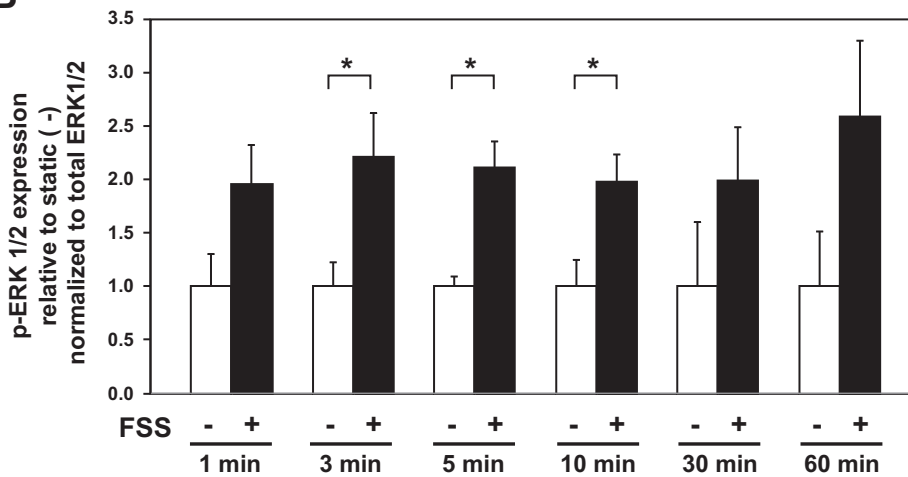


Fig. 2. Immunolocalization of occludin, ZO-1, and F-actin in murine cortical collecting duct (CCD; mpkCCD) cells exposed to fluid shear stress (FSS; 0.4 dyne/cm², 30 min) or circumferential stretch (CS; 10% equibiaxial stretch, 30 min). The tight junction protein occludin (*A–D*) and associated protein zonula occludens (ZO)-1 (*E–H*) localize to the plasma membrane of cells grown on glass (for FSS) or collagen IV-coated silicone supports (for CS) and show no change in localization after FSS or CS. Apical F-actin (*I–L*) localization in cells grown on glass or silicone was also not altered by FSS or CS. In contrast, mpkCCD cells showed prominent basolateral F-actin stress fibers after FSS (*N*), but enhanced membrane localization after CS (*P*).

A Cells grown on glass slides



B



C Cells grown on collagen coated glass slides

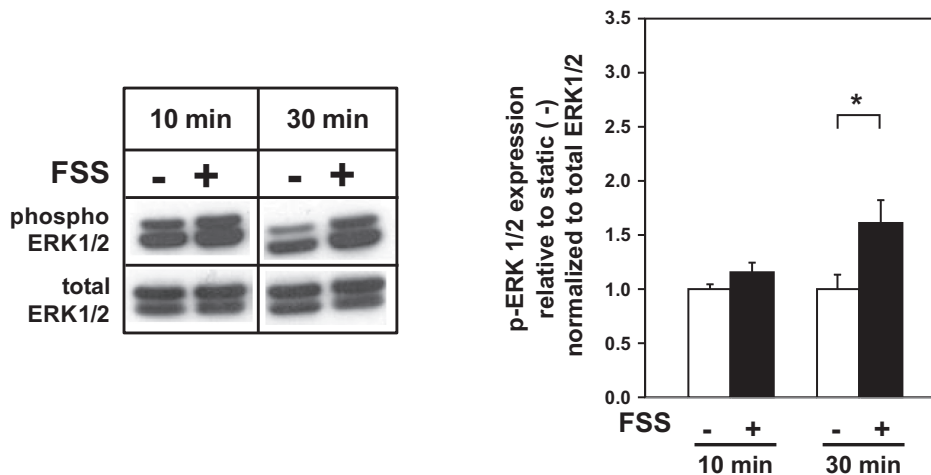


Fig. 3. FSS (0.4 dyne/cm²) induces pERK steady-state expression in mpkCCD cells grown on glass or collagen type IV-coated glass. *A*: representative Western blots of lysates of mpkCCD cells, grown on glass slides and exposed to FSS (+) or static (-) conditions for 1–60 min and probed for phosphorylated and total ERK. *B*: densitometric analysis of Western blots showing the mean of at least 4 individual experiments. Phosphorylation of ERK was apparent by 3 min of FSS. *C*: representative immunoblot (*right*) of protein lysate originating from mpkCCD cells grown on collagen IV-coated glass slides and exposed to FSS (+) or static (-) conditions for 10 or 30 min and probed for phosphorylated and total ERK. Densitometric analysis (*left*) demonstrates similar expression of p-ERK in static (*n* = 3) and FSS (*n* = 3)-exposed cells at 10 min, but steady-state abundance of p-ERK was significantly greater (**P* < 0.05) in FSS-exposed (*n* = 4) than static (*n* = 4) cells at 30 min. Values are means ± SE. **P* < 0.05 vs. static.

noblotting of cell lysates isolated from stretched and static cells with antibodies directed against pERK and p-p38 revealed that stretch was without significant effect on pERK expression (Fig. 5). When evaluating all phosphorylated isoforms of p38, CS did not affect net p-p38 expression compared with unstretched controls (Fig. 6, *A* and *B*). However, analysis of the low-molecular-weight p-p38 band alone revealed a $43.0 \pm 3.6\%$ reduction in expression (Fig. 6C) (**P* < 0.05) while expression of the high-molecular-weight band of p-p38 tended to increase (6.6 ± 2.8 fold; *P* < 0.1) in stretched cells. These

data suggest that stretch 1) does not affect the net expression of p-ERK or p-p38, but that stretch 2) stimulates selective/differential dephosphorylation and phosphorylation of unique p38 isoforms.

To address the concern that CS could lead to cell death and nonspecific signaling activation, mpkCCD cells were subjected to CS, as described in MATERIALS AND METHODS, and then exposed to trypan blue (an intravital dye) for assessment of cell viability (total viable cells/total cells). The cell viability in control ($89.0 \pm 1.2\%$ viable cells/insert; *n* = 6 inserts) and

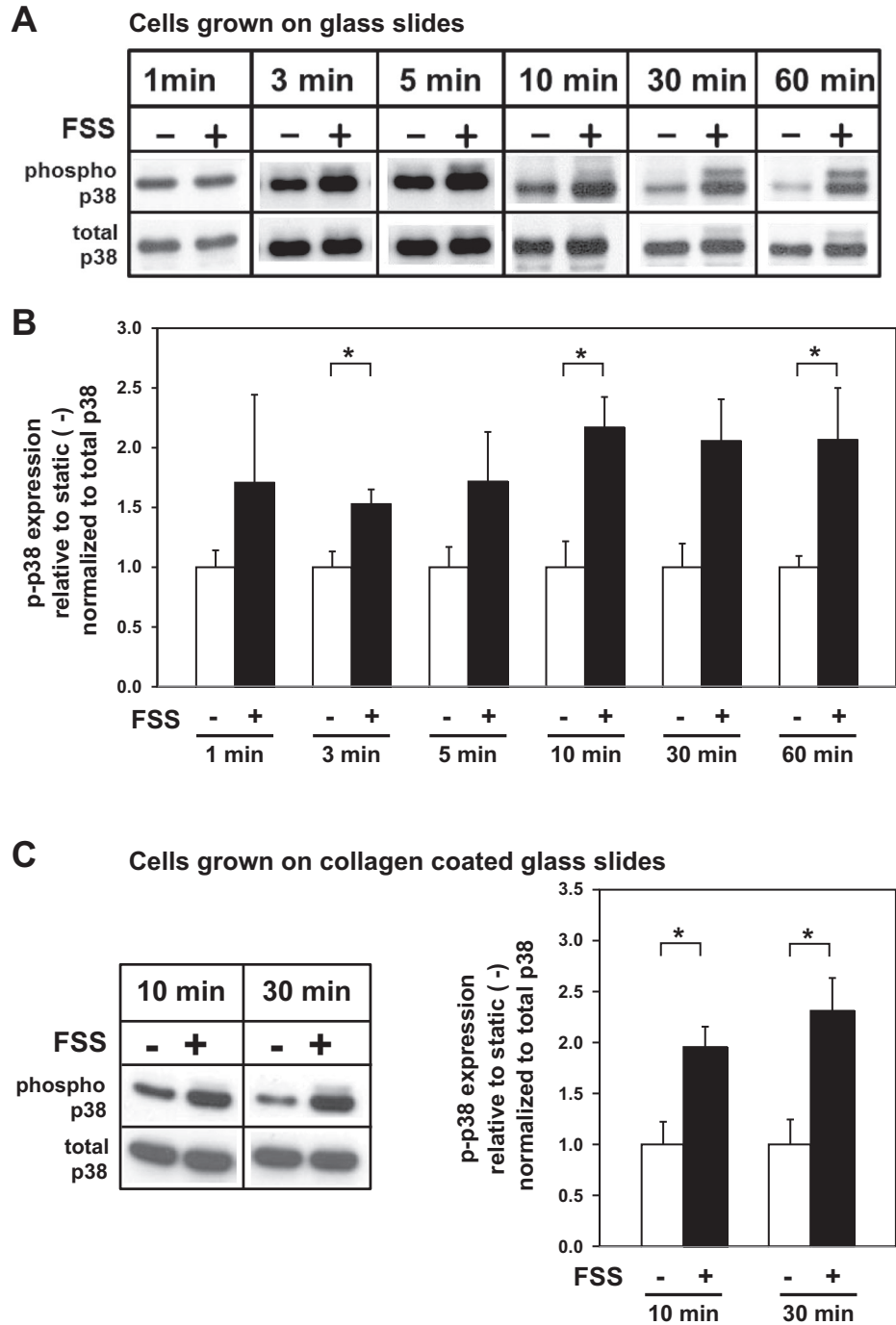


Fig. 4. FSS (0.4 dyne/cm²) induces p-p38 steady-state expression in mpkCCD cells grown on glass or collagen type IV-coated glass. *A*: representative Western blots of lysates of mpkCCD cells, grown on glass slides, exposed to FSS (+) or static (-) conditions for 1–60 min and probed for phosphorylated and total p38. *B*: densitometric analysis of Western blots showing the mean of at least 4 individual experiments. Phosphorylation of p38 was apparent within 3 min of FSS. *C*: representative immunoblot (*right*) of protein lysate originating from mpkCCD cells grown on collagen IV-coated glass slides and exposed to FSS (+) or static (-) conditions for 10 or 30 min and probed for phosphorylated and total p38. Densitometric analysis (*left*) demonstrates that p-p38 expression was significantly greater (**P* < 0.05) in FSS-exposed cells compared with static cells at 10 (*n* = 3) and 30 min (*n* = 4). Values are means ± SE. **P* < 0.05 vs. static.

stretched (90.7 ± 0.8% viable cells/insert; *n* = 6 inserts) cells did not differ.

CS Suppresses PGE₂ Release

We have previously reported that mpkCCD cells release PGE₂ into the media bathing cells in response to FSS of 0.4 dyne/cm² (13). Next, we tested whether CS leads to a similar release of PGE₂ into the media as observed in sheared cells. mpkCCD cells were exposed to the same 10% stretch stimulus for 30 min as described above, and PGE₂ concentration was measured in the media bathing the cells. As summarized in Fig. 7, PGE₂ release, normalized to total

cellular protein obtained from the well, was ~40% lower in cells exposed to CS (0.59 ± 0.05 pg·ml⁻¹·μg protein⁻¹; #*P* < 0.05) than that measured in unstretched static cells (1.00 ± 0.11 pg·ml⁻¹·μg protein⁻¹). These results suggest that CS inhibits PGE₂ release from renal epithelial cells, a response opposite to that elicited by FSS.

DISCUSSION

An acute increase in tubular fluid flow rate in the isolated perfused CCD leads to an increase in tubular diameter (~15%), [Ca²⁺]_i, epithelial sodium channel (ENaC)-mediated Na reabsorption, and FIKS. Flow activation of ENaC is due

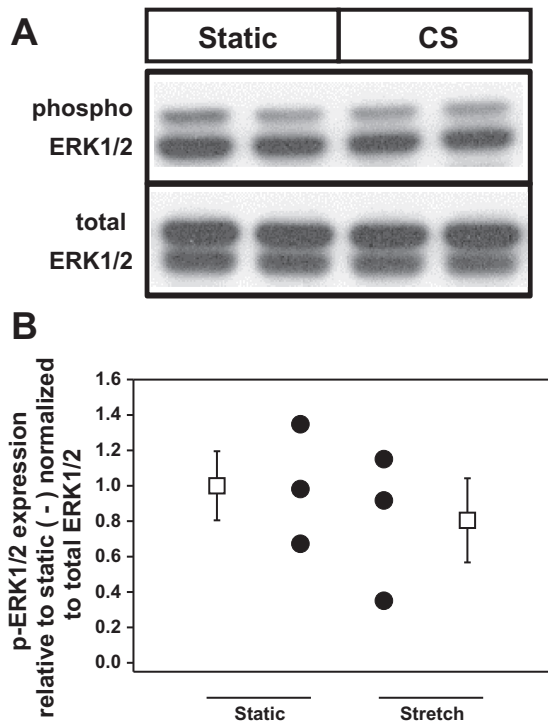


Fig. 5. Stretch (10%) does not affect pERK expression. *A*: representative Western blots of lysates of mpkCCD cells exposed to 10% CS for 30 min or to static conditions. *B*: densitometric analysis of Western blots showing individual and means \pm SE data for 3 individual experiments.

to an increase in channel open probability, mechanotransduced through the second transmembrane region of the α -subunit (1, 6); this flow-stimulated increase in ENaC activity may be tempered by flow-induced autocrine/paracrine signaling by extracellular nucleotides (38), PGE₂ (13), or endothelin-1 (24).

FIKS is a secretory flux mediated by the stretch- and Ca²⁺-activated BK channel (21, 23, 39, 40). The BK channel in principal cells is tonically inhibited by MAPK, p38, and ERK (17) as well as PKA (22). These observations suggest that hydrodynamic forces generated by increases in tubular fluid flow, which include FSS, CS, and drag/torque on apical cilia of Na-absorbing principal cells, activate/inhibit cell-specific signaling pathways that influence apical BK channel function. It is well established that mechanical manipulation of the cilium, as occurs with an increase in luminal flow rate (36), leads to an increase in Ca²⁺ influx (23, 26, 31–33), a signal expected to activate the BK channel. However, studies in IMCD3 cells in culture reveal that FSS induces phosphorylation (and activation) of ERK (12), an effector anticipated to inhibit the BK channel. The role of CS in renal tubular biology, signaling, and regulation of transepithelial transport remains relatively unexplored and was the focus of this investigation. Our results indicate that CS is a physiologically relevant mechanical force in the distal nephron in vivo in response to volume expansion or administration of loop diuretics and that CS and FSS differentially affect signaling pathways (MAPK and PGE₂ release) in mpkCCD cells, a model of the principal cell. While the focus of this manuscript has been on biomechanical signaling in principal cells, the CCD is composed of both principal and intercalated cells, both of which possess apical BK

channels. We acknowledge that hydrodynamic forces in the CCD may differentially affect signaling in intercalated and principal cells, a possibility that was not addressed in this investigation.

Although interest in the mechanoregulation of renal epithelial cell function has been increasing, little is known about the hydrodynamic forces prevailing in vivo in the native kidney. Micropuncture studies in the rat kidney have demonstrated that the tubular compliance (slope of the relationship between tubular diameter and intratubular pressure) of proximal and distal tubules differs in that it is linear in the former and a

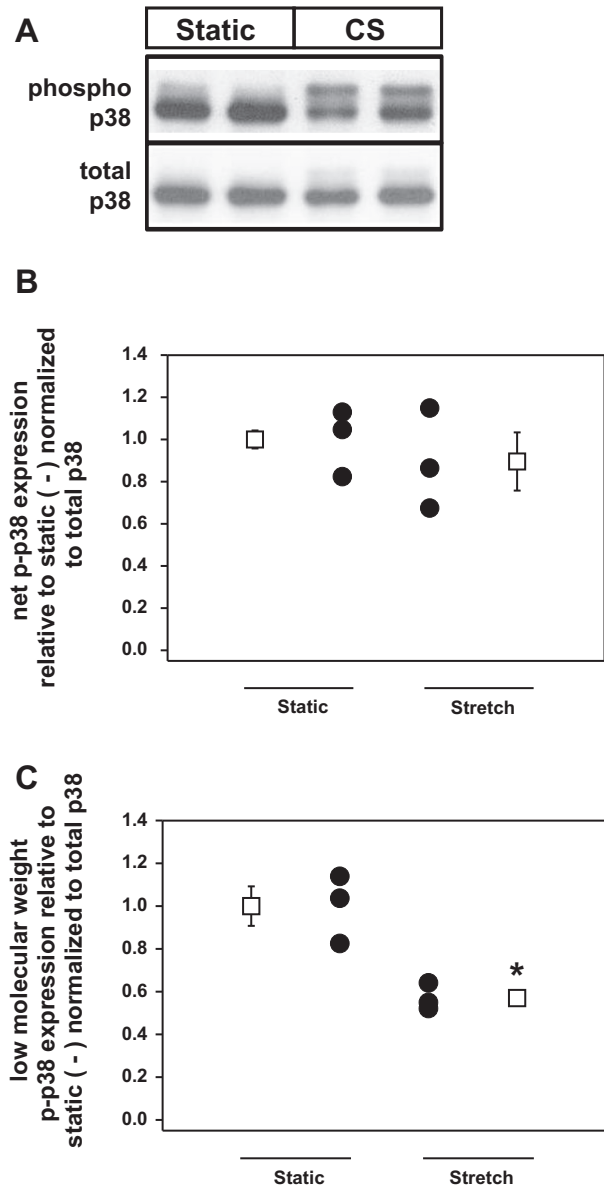


Fig. 6. Stretch (10%) differentially affects p-p38 expression. *A*: representative Western blots of lysates of mpkCCD cells exposed to 10% CS for 30 min or to static conditions. *B*: densitometric analysis (includes both bands of p-p38) of Western blots showing the individual and means \pm SE data for 3 individual experiments. CS did not alter the net steady-state phosphorylation of p38. *C*: densitometric analysis of the low-molecular-weight band of p-p38 demonstrates a significant reduction in p-p38 expression in CS-exposed cells vs. static cells. Values are means \pm SE (**P* < 0.05, vs. static). The absence of SE bars indicates that SE is smaller than the symbol.

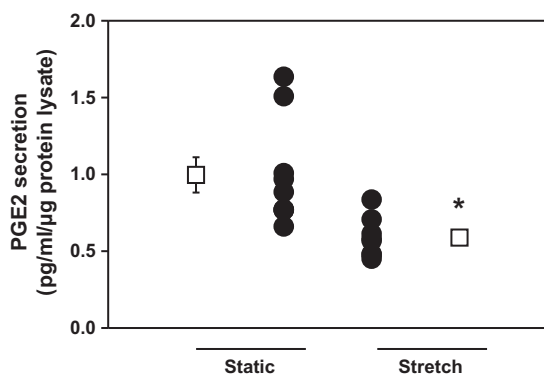


Fig. 7. Stretch (10%) suppresses PGE₂ release by mpkCCD cells. mpkCCD cells grown on collagen type IV-coated silicone supports for 7 days were exposed to no or 10% CS for 30 min. The PGE₂ concentration was measured in the media bathing the cells and normalized to the total amount of cellular protein lysate. Individual and means \pm SE (* P < 0.05 vs. static) data are shown in >8 experiments. The absence of SE bars indicates that SE is smaller than the symbol.

curvilinear in the latter (8); in the distal tubule, tubular diameter doubled in response to a 5-mmHg increase in tubular pressure but then increased by ever smaller amounts with progressively larger increases in tubular pressure. Utilizing a micropuncture approach, these same investigators further demonstrated that isotonic saline infusion caused a very small change in proximal tubular diameter (\sim 10%) but a much larger change to distal tubular diameter (\sim 40%) (11). While informative, results of micropuncture studies must be interpreted in the context that function and integrity of the tubule may be compromised when it is punctured (and injected with dye, oil, etc.). To better define hydrodynamic forces prevailing *in vivo*, we and others are now utilizing the less invasive approach of multiphoton microscopy to perform intravital imaging in intact rodent kidney. In fact, Kang et al. (15) used a quantitative imaging approach to study basic renal functions in the mouse and confirmed that furosemide administration produced a rapid increase in distal tubular diameter; however, the investigators did not quantify this change. The current study now extends the observations to demonstrate the magnitude of CS that can occur in the native rodent kidney distal nephron in response to volume expansion ($46.5 \pm 2.0\%$) or a furosemide-induced diuresis ($170 \pm 32\%$) (Fig. 1). A possible limitation of these findings, compared with those determined utilizing micropuncture, is that we are unable to completely exclude the possibility that some distal nephrons may be partially or minimally collapsed at the beginning of the experiment, before furosemide or saline infusion, thus making the percent change in diameter after the intervention even greater. We attempted to mitigate these concerns by 1) permitting animals access to food and water *ad libitum*, 2) immediately infusing a saline/Hoechst solution (\sim 400 μ l) bolus (to label nuclei) followed by a 300- μ l saline flush after lines are placed, and 3) overall, minimizing the time to perform the entire experiment to <1 h. These interventions at the beginning of the experiment would tend to equalize the volume status of all rodents and, therefore, limit the collapse of tubules.

We speculate that rapid expansion of distal tubular diameter may be accomplished by the apparent collapse of the microvasculature, as well as some tubules, presumably proximal

tubules (identified by their punctate endocytic uptake of the red dextran), after saline expansion and furosemide injection, which likely allows for the volume of the neighboring distal tubules to increase in the absence of an increase in total renal volume. In fact, the compression of peritubular capillaries by expanding tubules has been proposed to occur in the mice administered furosemide (28). Additional intravital imaging studies focused on the proximal tubule and peritubular capillaries will be necessary to rigorously examine this notion.

In vitro studies of epithelial cells, including proximal tubule cells, demonstrate that mechanical stimuli activate various intracellular and autocrine/paracrine signaling pathways and lead to rearrangement of the cytoskeleton or focal contacts (9). We have previously shown in a cell culture model of IMCD3 cells that FSS stimulates MAPK (ERK, p38, and JNK) signaling which, in turn, stimulates phosphorylation of cytosolic phospholipase A₂ and cyclooxygenase (COX)-2 expression (12, 13). The net effect of FSS activation of these cellular pathways is robust secretion of PGE₂ which, we demonstrate, in *ex vivo* microperfused rabbit CCDs, inhibits Na absorption and stimulates K secretion (13).

We now show that PGE₂ secretion/release was stimulated by FSS, but suppressed by CS. Net steady-state abundance of pERK and p-p38 were unchanged by CS; however, we found that CS selectively suppressed the abundance of the lower molecular weight isoform of p-p38 while tending to enhance the expression of the higher molecular weight p-p38. In addition, FSS induced actin stress fibers at the basolateral membrane, but CS tended to relocate actin to the lateral membrane. These studies illustrate that biomechanical forces differentially effectuate intracellular and paracrine signaling, as well as cytoskeletal organization, in the distal nephron.

Alexander et al. (3) tested whether varying levels of stretch and durations of stretch regulated MAPK activation and PGE₂ release utilizing primary cultures of rabbit proximal tubule cells. This group found that increasing duration and degree of stretch stimulated ERK phosphorylation, cPLA2 phosphorylation, and PGE₂ release (3), implying that rabbit proximal tubular cells behave differently than our murine CCD cells. Technical considerations limit direct comparison of the former results with those in the current investigation, since Alexander et al. grew their cells on type I collagen, used a uniaxial elongation chamber (Flexercell Strain Unit) to subject their cells to 30 rounds of cyclic stretch/min, and exposed the cells from 2 to 20% stretch (3). Note that our studies show that pERK was unaffected and PGE₂ was suppressed by CS. The conditions we chose to deliver CS (10% constant equibiaxial stretch \times 30 min) are based on our *ex vivo* and *in vivo* observations of the effects of increases in tubular flow in the distal nephron.

Studies in cultured renal epithelial cells have shown that FSS triggers signaling events, such as increases in $[Ca^{2+}]_i$, through mechanical deformation of the actin cytoskeleton and focal adhesion complexes (2). Duan et al. (9) demonstrated that FSS promotes cytoskeletal reorganization in proximal tubular cells by 1) redistributing stress fibers from the basolateral membrane to the apical surface and 2) forming new apical junctional complexes. In contrast, we found that F-actin stress fiber expression increased at the basolateral surface of mpkCCD cells in response to FSS and lateral surfaces of the cell-cell interface of CS exposed cells. However, neither FSS nor CS

significantly altered localization of tight junctional proteins. We speculate that FSS- and CS-induced reorganization of the cytoskeleton reflects downstream activation of effectors including focal adhesion kinase (FAK) (19) and MAPK pathways, as described by Peng et al. (18) in an osteoblastic cell line.

Obstructive uropathy, a cause of acute kidney injury, is associated with tubular stretch, intratubular pressure, and elevated urinary PGE₂, which contributes to postobstructive diuresis by suppressing renal Na transporter and aquaporin expression (16, 25, 27). Studies presented in this paper suggest that CS of the CCD reduces PGE₂ secretion, which differs from the observation in the hydronephrosis model. This difference may be explained by the fact that multiple biomechanical forces, other than CS, come into play in obstructive uropathy, such as hydrostatic pressure, which were not studied in the present investigation. In fact, several investigators have demonstrated that increases in intrarenal pressure stimulate COX-2 expression in interstitial cells, but not in the collecting duct, to induce PGE₂ expression (7, 27). Therefore, because of the complexity of cell types and mechanical forces present in the hydronephrotic kidney, it is difficult to directly extrapolate our current findings to the hydronephrosis model. However, we speculate that CS inhibits tubular PGE₂ secretion while other cell types (i.e., interstitial cells) generate more PGE₂, leading to the net effect of high PGE₂ concentrations in hydronephrosis.

In summary, our findings of 1) CS in the intact mammalian kidney in the face of increases in distal tubular flow and 2) differential effects of FSS and CS on MAPK activation and PGE₂ release in mpkCCD cells challenge the notion previously put forth by ourselves and others that FSS and cilia-mediated mechanotransduction are the sole physiologically relevant hydrodynamic forces in the distal nephron *in vivo*. Indeed, CS is a particularly attractive candidate for a biomechanical force regulating CCD function, as its effect on p-p38 abundance (reduction in the low-molecular-weight band) may account for activation of BK channel-mediated K secretion in CCDs subject to an increase in tubular fluid flow. However, we acknowledge that the net effect of an increase in tubular fluid flow on epithelial cell function in the distal nephron will represent the integration of pathways activated by FSS, CS, as well as drag/torque on the apical cilia and microvilli/microplacae of principal and intercalated cells, respectively, therein.

ACKNOWLEDGMENTS

Image collection and digital image analysis were conducted at the Microscopy Shared Resource Facility at the Icahn School of Medicine at Mount Sinai and the Indiana Center for Biological Microscopy.

GRANTS

This work was supported by a Department of Veterans Affairs Merit Review 1I01BX000388 (R. Rohatgi), R01DK83470 (L. M. Satlin), DK51391 (T. R. Kleyman), the Pittsburgh Center for Kidney Research (DK079307; T. R. Kleyman), George M. O'Brien Award (DK61594; B. A. Molitoris), R01EB006834 (F. Y. Lee), and R01AR056246 (F. Y. Lee).

DISCLOSURES

No conflicts of interest, financial or otherwise, are declared by the authors.

AUTHOR CONTRIBUTIONS

Author contributions: R.C.-G., R.M.S., L.M.S., and R.R. provided conception and design of research; R.C.-G., Y.L., D.F., C.E., H.G.L., G.J.R., and

R.M.S. performed experiments; R.C.-G., R.M.S., L.M.S., and R.R. analyzed data; R.C.-G., L.M.S., and R.R. interpreted results of experiments; R.C.-G. prepared figures; R.M.S., T.R.K., F.Y.L., B.A.M., L.M.S., and R.R. edited and revised manuscript; L.M.S. and R.R. approved final version of manuscript; R.R. drafted manuscript.

REFERENCES

1. **Abi-Antoun T, Shi S, Tolino LA, Kleyman TR, Carattino MD.** Second transmembrane domain modulates epithelial sodium channel gating in response to shear stress. *Am J Physiol Renal Physiol* 300: F1089–F1095, 2011.
2. **Alenghat FJ, Nauli SM, Kolb R, Zhou J, Ingber DE.** Global cytoskeletal control of mechanotransduction in kidney epithelial cells. *Exp Cell Res* 301: 23–30, 2004.
3. **Alexander LD, Alagarsamy S, Douglas JG.** Cyclic stretch-induced cPLA2 mediates ERK 1/2 signaling in rabbit proximal tubule cells. *Kidney Int* 65: 551–563, 2004.
4. **Ashworth SL, Sandoval RM, Tanner GA, Molitoris BA.** Two-photon microscopy: visualization of kidney dynamics. *Kidney Int* 72: 416–421, 2007.
5. **Bailey MA, Cantone A, Yan Q, MacGregor GG, Leng Q, Amorim JB, Wang T, Hebert SC, Giebisch G, Malnic G.** Maxi-K channels contribute to urinary potassium excretion in the ROMK-deficient mouse model of Type II Bartter's syndrome and in adaptation to a high-K diet. *Kidney Int* 70: 51–59, 2006.
6. **Carattino MD, Sheng S, Kleyman TR.** Epithelial Na⁺ channels are activated by laminar shear stress. *J Biol Chem* 279: 4120–4126, 2004.
7. **Carlsen I, Donohue KE, Jensen AM, Selzer AL, Chen J, Poppas DP, Felsen D, Frøkiær J, Nørregaard R.** Increased cyclooxygenase-2 expression and prostaglandin E₂ production in pressurized renal medullary interstitial cells. *Am J Physiol Regul Integr Comp Physiol* 299: R823–R831, 2010.
8. **Cortell S, Gennari FJ, Davidman M, Bossert WH, Schwartz WB.** A definition of proximal and distal tubular compliance. Practical and theoretical implications. *J Clin Invest* 52: 2330–2339, 1973.
9. **Duan Y, Gotoh N, Yan Q, Du Z, Weinstein AM, Wang T, Weinbaum S.** Shear-induced reorganization of renal proximal tubule cell actin cytoskeleton and apical junctional complexes. *Proc Natl Acad Sci USA* 105: 11418–11423, 2008.
10. **Dunn KW, Sandoval RM, Kelly KJ, Dagher PC, Tanner GA, Atkinson SJ, Bacallao RL, Molitoris BA.** Functional studies of the kidney of living animals using multicolor two-photon microscopy. *Am J Physiol Cell Physiol* 283: C905–C916, 2002.
11. **Fitzgibbons JP, Gennari FJ, Garfinkel HB, Cortell S.** Dependence of saline-induced natriuresis upon exposure of the kidney to the physical effects of extracellular fluid volume expansion. *J Clin Invest* 54: 1428–1436, 1974.
12. **Flores D, Battini L, Gusella GL, Rohatgi R.** Fluid shear stress induces renal epithelial gene expression through polycystin-2-dependent trafficking of extracellular regulated kinase. *Nephron Physiol* 117: p27–36, 2011.
13. **Flores D, Liu Y, Liu W, Satlin LM, Rohatgi R.** Flow-induced prostaglandin E₂ release regulates Na and K transport in the collecting duct. *Am J Physiol Renal Physiol* 303: F632–F638, 2012.
14. **Gutierrez-Sanmartin D, Varela-Ledo E, Aguilera A, Romero-Yuste S, Romero-Jung P, Gomez-Tato A, Regueiro BJ.** Implication of p38 mitogen-activated protein kinase isoforms (alpha, beta, gamma and delta) in CD4⁺ T-cell infection with human immunodeficiency virus type I. *J Gen Virol* 89: 1661–1671, 2008.
15. **Kang JJ, Toma I, Sipos A, McCulloch F, Peti-Peterdi J.** Quantitative imaging of basic functions in renal (patho)physiology. *Am J Physiol Renal Physiol* 291: F495–F502, 2006.
16. **Kuhl PG, Schonig G, Schwehr H, Seyberth HW.** Increased renal biosynthesis of prostaglandin E₂ and thromboxane B₂ in human congenital obstructive uropathy. *Pediatr Res* 27: 103–107, 1990.
17. **Li D, Wang Z, Sun P, Jin Y, Lin DH, Hebert SC, Giebisch G, Wang WH.** Inhibition of MAPK stimulates the Ca²⁺-dependent big-conductance K channels in cortical collecting duct. *Proc Natl Acad Sci USA* 103: 19569–19574, 2006.
18. **Li P, Ma YC, Shen HL, Han H, Wang J, Cheng HJ, Wang CF, Xia YY.** Cytoskeletal reorganization mediates fluid shear stress-induced ERK5 activation in osteoblastic cells. *Cell Biol Int* 36: 229–236, 2012.
19. **Li S, Kim M, Hu YL, Jalali S, Schlaepfer DD, Hunter T, Chien S, Shyy JY.** Fluid shear stress activation of focal adhesion kinase. Linking to mitogen-activated protein kinases. *J Biol Chem* 272: 30455–30462, 1997.

20. **Ling BN, Webster CL, Eaton DC.** Eicosanoids modulate apical Ca^{2+} -dependent K^+ channels in cultured rabbit principal cells. *Am J Physiol Renal Fluid Electrolyte Physiol* 263: F116–F126, 1992.
21. **Liu W, Morimoto T, Woda C, Kleyman TR, Satlin LM.** Ca^{2+} dependence of flow-stimulated K^+ secretion in the mammalian cortical collecting duct. *Am J Physiol Renal Physiol* 293: F227–F235, 2007.
22. **Liu W, Wei Y, Sun P, Wang WH, Kleyman TR, Satlin LM.** Mechano-regulation of BK channel activity in the mammalian cortical collecting duct: role of protein kinases A and C. *Am J Physiol Renal Physiol* 297: F904–F915, 2009.
23. **Liu W, Xu S, Woda C, Kim P, Weinbaum S, Satlin LM.** Effect of flow and stretch on the $[\text{Ca}^{2+}]_i$ response of principal and intercalated cells in cortical collecting duct. *Am J Physiol Renal Physiol* 285: F998–F1012, 2003.
24. **Lyon-Roberts B, Strait KA, van Peurse E, Kittikuluth W, Pollock JS, Pollock DM, Kohan DE.** Flow regulation of collecting duct endothelin-1 production. *Am J Physiol Renal Physiol* 300: F650–F656, 2011.
25. **Murer L, Addabbo F, Carmosino M, Procino G, Tamma G, Montini G, Rigamonti W, Zucchetto P, Della Vella M, Venturini A, Zacchello G, Svelto M, Valenti G.** Selective decrease in urinary aquaporin 2 and increase in prostaglandin E2 excretion is associated with postobstructive polyuria in human congenital hydronephrosis. *J Am Soc Nephrol* 15: 2705–2712, 2004.
26. **Nauli SM, Alenghat FJ, Luo Y, Williams E, Vassilev P, Li X, Elia AE, Lu W, Brown EM, Quinn SJ, Ingber DE, Zhou J.** Polycystins 1 and 2 mediate mechanosensation in the primary cilium of kidney cells. *Nat Genet* 33: 129–137, 2003.
27. **Nørregaard R, Jensen BL, Li C, Wang W, Knepper MA, Nielsen S, Frøkiær J.** COX-2 inhibition prevents downregulation of key renal water and sodium transport proteins in response to bilateral ureteral obstruction. *Am J Physiol Renal Physiol* 289: F322–F333, 2005.
28. **Oppermann M, Hansen PB, Castrop H, Schnermann J.** Vasodilatation of afferent arterioles and paradoxical increase of renal vascular resistance by furosemide in mice. *Am J Physiol Renal Physiol* 293: F279–F287, 2007.
29. **Pluznick JL, Wei P, Carmines PK, Sansom SC.** Renal fluid and electrolyte handling in $\text{BK}_{\text{Ca}}\text{-}\beta 1\text{-}/\text{-}$ mice. *Am J Physiol Renal Physiol* 284: F1274–F1279, 2003.
30. **Pluznick JL, Wei P, Grimm PR, Sansom SC.** BK- $\beta 1$ subunit: immunolocalization in the mammalian connecting tubule and its role in the kaliuretic response to volume expansion. *Am J Physiol Renal Physiol* 288: F846–F854, 2005.
31. **Praetorius HA, Spring KR.** Bending the MDCK cell primary cilium increases intracellular calcium. *J Membr Biol* 184: 71–79, 2001.
32. **Praetorius HA, Spring KR.** Removal of the MDCK cell primary cilium abolishes flow sensing. *J Membr Biol* 191: 69–76, 2003.
33. **Praetorius HA, Spring KR.** The renal cell primary cilium functions as a flow sensor. *Curr Opin Nephrol Hypertens* 12: 517–520, 2003.
34. **Rieg T, Vallon V, Sausbier M, Sausbier U, Kaissling B, Ruth P, Osswald H.** The role of the BK channel in potassium homeostasis and flow-induced renal potassium excretion. *Kidney Int* 72: 566–573, 2007.
35. **Sandoval RM, Wagner MC, Patel M, Campos-Bilderback SB, Rhodes GJ, Wang E, Wean SE, Clendenon SS, Molitoris BA.** Multiple factors influence glomerular albumin permeability in rats. *J Am Soc Nephrol* 23: 447–457, 2012.
36. **Schwartz EA, Leonard ML, Bizios R, Bowser SS.** Analysis and modeling of the primary cilium bending response to fluid shear. *Am J Physiol Renal Physiol* 272: F132–F138, 1997.
37. **Svenningsen P, Burford JL, Peti-Peterdi J.** ATP releasing connexin 30 hemichannels mediate flow-induced calcium signaling in the collecting duct. *Front Physiol* 4: 292, 2013.
38. **Vallon V, Stockand J, Rieg T.** P2Y receptors and kidney function. *Wiley Interdiscip Rev Membr Transp Signal* 1: 731–742, 2012.
39. **Weinbaum S, Duan Y, Satlin LM, Wang T, Weinstein AM.** Mechano-transduction in the renal tubule. *Am J Physiol Renal Physiol* 299: F1220–F1236, 2010.
40. **Woda CB, Bragin A, Kleyman TR, Satlin LM.** Flow-dependent K^+ secretion in the cortical collecting duct is mediated by a maxi-K channel. *Am J Physiol Renal Physiol* 280: F786–F793, 2001.
41. **Woda CB, Miyawaki N, Ramalakshmi S, Ramkumar M, Rojas R, Zavilowitz B, Kleyman TR, Satlin LM.** Ontogeny of flow-stimulated potassium secretion in rabbit cortical collecting duct: functional and molecular aspects. *Am J Physiol Renal Physiol* 285: F629–F639, 2003.